Composition-Tunable Zn$_x$Cd$_{1-x}$Se Nanocrystals with High Luminescence and Stability

Xinhua Zhong,[†] Mingyong Han,*,[†,‡] Zhili Dong,[§] Timothy J. White,[§] and Wolfgang Knoll*,[†]

Contribution from the Department of Materials Science and Department of Chemistry, National University of Singapore, Singapore 117543, Institute of Materials Research and Engineering, 3 Research Link, Singapore 117602, and Institute of Environmental Science and Engineering, 18 Nanyang Drive, Singapore 637723

Received March 11, 2003; E-mail: mashanmy@nus.edu.sg

Abstract: High-quality Zn$_x$Cd$_{1-x}$Se nanocrystals have been successfully prepared at high temperature by incorporating stoichiometric amounts of Zn and Se into pre-prepared CdSe nanocrystals. With increasing Zn content, a composition-tunable emission across most of the visible spectrum has been demonstrated by a systematic blue-shift in emission wavelength. The photoluminescence (PL) properties for the obtained Zn$_x$Cd$_{1-x}$Se nanocrystals (PL efficiency of 70−85%, fwhm = 22−30 nm) are comparable to those for the best reported CdSe-based QDs. In particular, they also have good PL properties in the blue spectral range. Moreover, the alloy nanocrystals can retain their high luminescence (PL efficiency of over 40%) when dispersed in aqueous solutions and maintain a symmetric peak shape and spectral position under rigorous experimental conditions. A rapid alloying process was observed at a temperature higher than "alloying point". The mechanism of the high luminescence efficiency and stability of Zn$_x$Cd$_{1-x}$Se nanocrystals is explored.

Introduction

Colloidal semiconductor nanocrystals, also known as quantum dots (QDs), are of tremendous fundamental and technical interest due to their applications as light-emitting devices,[1,2] lasers,[3,4] and biological labels.[5−8] Owing to their size-dependent photoluminescence (PL) tunable across the visible spectrum, CdSe nanocrystals have become the most extensively investigated QDs.[9−13] A major problem encountered over the years in fabricating high-quality QDs is associated with materials issues, primarily the tendency to form defects and surface-trap states under the employed growth conditions, resulting in low luminescence efficiency and stability deficits. Surface-passivation of the CdSe nanocrystals with suitable organic or inorganic materials can minimize this problem by removing the non-radiative recombination centers. The best PL efficiency reported for CdSe QDs can reach over 50% in the wavelength window above 520 nm, but the efficiency for the blue spectral range is still low.[13−18] Organic passivation is often incomplete or reversible. The luminescence intensity of organically passivated CdSe nanocrystals will dramatically decrease when capping materials (such as alkylamine or trioctylphosphine oxide) are displaced in order to render them water-soluble. This limits their functionality in biomedical labeling application. Effective inorganic-passivation can form core−shell structured QDs (such as CdSe/ZnS and CdSe/CdS) that are more robust than the organic-coated QDs against chemical degradation or photo-oxidation.[14−16] However, for the largely mismatched core−shell structures, the interface strain accumulates dramatically with increasing shell thickness, and eventually can be released through the formation of misfit dislocations, degrading the optical properties of the QDs. Consequently, it remains a major goal to develop new synthetic methods or strategies of producing highly luminescent stable QDs, especially blue-emitting ones.

* To whom correspondence should be addressed.
† National University of Singapore.
‡ Institute of Materials Research and Engineering.
§ Institute of Environmental Science and Engineering.

(1) Colvin, V. L.; Schlamp, M. C.; Alivisatos, A. P. *Nature* **1994**, *370*, 354.
(2) Tessler, N.; Medvedev, V.; Kazes, M.; Kan, S. H.; Banin, U. *Science* **2002**, *295*, 1506.
(3) Klimov, V. I.; Mikhailovsky, A. A.; Xu, S.; Malko, A.; Hollingsworth, J. A.; Leatherdale, C. A.; Eisler, H. J.; Bawendi, M. G. *Science* **2000**, *290*, 314.
(4) Artemyev, M. V.; Woggon, U.; Wannemacher, R.; Jaschinski, H.; Langbein, W. *Nano Lett.* **2001**, *1*, 309.
(5) Bruchez, M.; Moronne, M.; Gin, P.; Weiss, S.; Alivisatos, A. P. *Science* **1998**, *281*, 2013.
(6) Chan, W. C. W.; Nie, S. M. *Science* **1998**, *281*, 2016.
(7) Han, M. Y.; Gao, X. H.; Su, J. Z.; Nie, S. M. *Nat. Biotechnol.* **2001**, *19*, 631.
(8) Chan, W. C. W.; Maxwell, D. J.; Gao, X. H.; Bailey, R. E.; Han, M. Y.; Nie, S. M. *Curr. Opin. Biotech.* **2002**, *13*, 40.
(9) Murray, C. B.; Norris, D. J.; Bawendi, M. G. *J. Am. Chem. Soc.* **1993**, *115*, 8706.
(10) Peng, X. *Chem. Eur. J.* **2002**, *8*, 334.
(11) Peng, Z. A.; Peng, X. *J. Am. Chem. Soc.* **2001**, *123*, 183.
(12) Qu, L.; Peng, Z. A.; Peng, X. *Nano Lett.* **2001**, *1*, 333.
(13) Qu, L.; Peng, X. *J. Am. Chem. Soc.* **2002**, 124, 2049.

(14) Hines, M. A.; Guyot-Sionnest, P. *J. Phys. Chem.* **1996**, *100*, 468.
(15) Peng, X.; Schlamp, M. C.; Kadavanich, A. V.; Alivisatos, A. P. *J. Am. Chem. Soc.* **1997**, *119*, 7019.
(16) Dabbousi, B. O.; Rodriguez-Viejo, J.; Mikulec, F. V.; Heine, J. R.; Mattoussi, H.; Ober, R.; Jensen, K. F.; Bawendi, M. G. *J. Phys. Chem. B* **1997**, *101*, 9463.
(17) Reiss, P.; Bleuse, J.; Pron, A. *Nano Lett.* **2002**, *2*, 781.
(18) Talapin, D. V.; Rogach, A. L.; Kornowski, A.; Haase, M.; Weller, H. *Nano Lett.* **2001**, *1*, 207.

In the last two decades, the main focus has been on the preparation of different color-emitting QDs with different particle sizes. Little attention has been paid to the fact that different color-emitting QDs can also be made through the control of constituent stoichiometries in alloy nanoparticles. Although bulk or thin film semiconductor alloys have been extensively investigated due to their wide application in optoelectronics,[19] only a limited number of studies have been reported for the preparation of alloy or composite nanocrystals by coprecipitation or slow diffusion of their constituents via wet chemistry routes.[20−24] Unfortunately, all these reported alloy or composite nanocrystals have poor PL properties.

In this study, an effective high-temperature synthetic strategy has been developed to make a series of high-quality $Zn_xCd_{1-x}Se$ alloy nanocrystals with emission wavelengths ranging from 460 to 630 nm by incorporating Zn and Se into pre-prepared starting CdSe nanocrystals. The composition-tunable emission across the visible spectrum has been systematically demonstrated over the composition of the $Zn_xCd_{1-x}Se$ nanocrystals (the emission wavelength blue-shifts gradually with the increase of Zn content). The resulting alloy nanocrystals have comparable PL properties to the best-reported CdSe-based QDs. In addition, they also have good PL properties in the blue spectral range and can retain their high luminescence when dispersed in aqueous solutions. Meanwhile, a rapid alloying process for the formation of homogeneous alloy nanocrystals was observed at a temperature above "alloying point". The high luminescence efficiency and stability of the resulting alloy nanocrystals are attributed to the larger particle size, higher crystallinity, higher covalency, lower inter-diffusion, and spatial composition fluctuation. The highly luminescent stable alloy nanocrystals, in particular, those that are blue-emitting, are potential ideal materials for light-emitting devices and quantum dot lasers, which could solve problems occurring in the promising, but highly strained, $Zn_xCd_{1-x}Se/ZnSe$ quantum-well structures. These alloy nanocrystals would also be a new class of biomedical labels for ultrasensitive, multicolor, and multiplexing applications.

Experimental Section

Chemicals. Trioctylphosphine oxide (TOPO, 99%), trioctylphosphine (TOP, 90%), octadecylamine (ODA, 90%), stearic acid (95%), diethylzinc ($ZnEt_2$, 1.0 M solution in heptane), and Se powder (99.999%) were purchased from Aldrich. CdO (99.999%) and cadmium stearate (90%) were purchased from Strem. Methanol, toluene, chloroform, and acetone were purchased from Merck.

Synthesis of $Zn_xCd_{1-x}Se$ Nanocrystals. All manipulations were performed using standard air-free techniques. Stock solutions for Se and $ZnEt_2$ were prepared in a glovebox under Ar. Most details of the synthetic and characterization methods were similar to those reported in the literature.[11−13]

Typically, 0.2044 g (0.3 mmol) of cadmium stearate, 0.1707 g (0.6 mmol) of stearic acid, 5.0 g of trioctylphosphine oxide (TOPO), and 5.0 g of octadecylamine (ODA) were added to a flask, and the mixture

was heated to 310−330 °C under Ar flow until a clear solution formed. At this temperature, an excess amount of Se solution containing 0.1184 g (1.5 mmol) of Se dissolved in 4.0 g of trioctylphosphine (TOP) was swiftly injected into the reaction flask, after which time the temperature was set at 270−300 °C. After 5−10 min, the heating was removed to stop the reaction and allow the flask to cool to room temperature. This cooling step is essential for the later incorporation of Zn/Se into the pre-prepared CdSe QDs.

A certain amount (3 mL) of the as-prepared crude CdSe reaction mixture containing 0.1 mmol of CdSe was reheated to 290−320 °C. At this temperature, $ZnEt_2$ solution (0.2 M) in TOP and Se solution (0.2 M) in TOP were added alternatively at time intervals of 20 s. After the addition, the reaction mixture was heated until no further PL peak shift (about 3−6 min), and then heat was removed to stop the reaction. The ratio of Zn/Cd in each targeted $Zn_xCd_{1-x}Se$ nanocrystals can be achieved by the alteration of the amounts of Zn and Se precursors. Blue-emitting alloy nanocrystals with shorter emission wavelength can be prepared by using smaller sized starting CdSe QDs.

Characterization of $Zn_xCd_{1-x}Se$ Nanocrystals. All the resulting samples were immediately cooled and diluted with chloroform. The UV−vis and PL spectra of the $Zn_xCd_{1-x}Se$ nanocrystals were recorded promptly. The room-temperature PL efficiencies were determined by comparing the integrated emission of the QDs samples to that of dyes in solutions with identical optical density at the excitation wavelength. The excitation wavelengths were set at the first absorption peak of the measured ODs. The dyes (such as rhodamine 6G, rhodamine 640, or coumarin 540) should have significantly overlaps in PL spectra with the QDs to be measured. A quadratic refractive index correction was done when two different solvents were used to dissolve QDs and dyes.[25] Also the known efficiencies of the QDs in chloroform can be used to measure the efficiencies of other QDs by comparing their integrated emission or PL intensity of solutions. A low concentration of solutions was used to avoid obvious reabsorption.

A mixed solvent of methanol and acetone was used to precipitate the resulting nanocrystals in chloroform solution, which were isolated by centrifugation and decantation. The excess ligands and reaction precursors were removed by extensive purification prior to high-resolution transmission electron microscopy (HRTEM), powder X-ray diffraction (XRD), and inductively coupled plasma atomic emission (ICP) measurements. No further size-selective purification was done for the samples. A JEOL JEM3010 transmission electron microscope (operated at an accelerating voltage of 300 kV) was used to analyze the size, size distribution, and structure of the resulting nanocrystals, which were deposited on Formvar/carbon-coated copper grids using the QD hexane solutions. The size distribution histograms for all the samples were obtained by analyzing over 200 crystallites in each sample. The XRD patterns of the final products were recorded by a Siemens D5005 X-ray powder diffractometer. The composition of the obtained $Zn_xCd_{1-x}Se$ nanocrystals was measured by means of ICP by a standard HCl/HNO_3 digestion.

Results and Discussion

Composition and Size Distribution. The composition-tunable $Zn_xCd_{1-x}Se$ nanocrystals were prepared by incorporating stoichiometric amounts of Zn and Se into the same batch of pre-prepared CdSe QDs at high temperature. The HRTEM in Figures 1 and 2 show nearly monodispersed $Zn_xCd_{1-x}Se$ nanocrystals, which have well-resolved lattice fringes and remain fully crystalline upon ZnSe incorporation. The particle size increases proportionally from 5.2 to 7.5 nm with the increase of Zn content from 0 to 0.67. The mole fraction of Zn in the resulting nanocrystals was determined by ICP method. This is in agreement with the estimation of ZnSe content in the

(19) Chen, A.-B.; Sher, A. *Semiconductor Alloys,* Plenum Press: New York, **1996**.
(20) Korgel, B. A.; Monbouquette, H. G. *Langmuir* **2000**, *16*, 3588.
(21) Petrov, D. V.; Santos, B. S.; Pereira, G. A. L.; Donegá, C. D. M. *J. Phys. Chem. B* **2002**, *106*, 5325.
(22) Harrison, M. T.; Kershaw, S. V.; Burt, M. G.; Eychmüller, A.; Weller, H.; Rogach, A. L. *Mater. Sci. Eng. B* **2000**, *69*, 355.
(23) Tian, Y.; Newton, T.; Kotov, N. A.; Guldi, D. M.; Fendler, J. H. *J. Phys. Chem.* **1996**, *100*, 8927.
(24) Wang, W.; Germanenko, I.; El-Shall, M. S. *Chem. Mater*. **2002**, *14*, 3028.
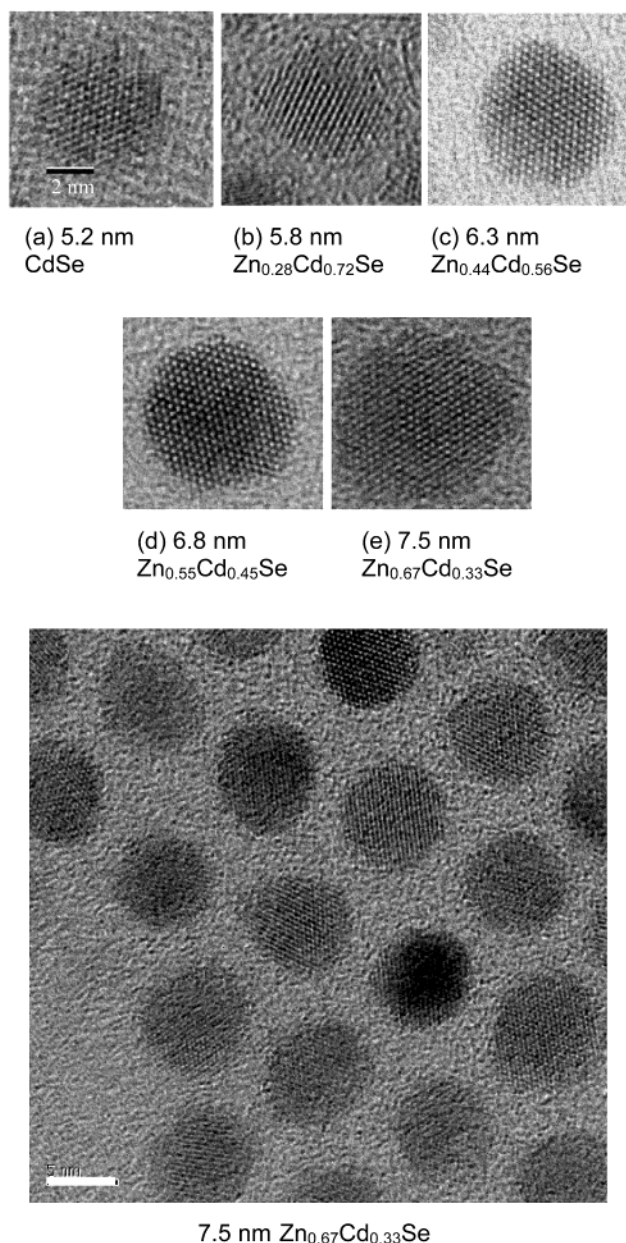
(25) Demas, J. N.; Crosby, G. A. *J. Phys. Chem.* **1971**, *75*, 991.

(a) 5.2 nm
CdSe

(b) 5.8 nm
Zn$_{0.28}$Cd$_{0.72}$Se

(c) 6.3 nm
Zn$_{0.44}$Cd$_{0.56}$Se

(d) 6.8 nm
Zn$_{0.55}$Cd$_{0.45}$Se

(e) 7.5 nm
Zn$_{0.67}$Cd$_{0.33}$Se

7.5 nm Zn$_{0.67}$Cd$_{0.33}$Se

Figure 1. HRTEM characterization for Zn$_x$Cd$_{1-x}$Se nanocrystals with Zn mole fractions of (a) 0, (b) 0.28, (c) 0.44, (d) 0.55, and (e) 0.67. Wide-field HRTEM micrograph (bottom) of Zn$_{0.67}$Cd$_{0.33}$Se nanocrystals (sample e). Scale bar = 5 nm.

Zn$_x$Cd$_{1-x}$Se nanocrystals by using the particle sizes determined by HRTEM (Figure 1). All the as-prepared Zn$_x$Cd$_{1-x}$Se nano-crystals with Zn mole fractions of 0, 0.28, 0.44, 0.55, and 0.67 have narrow size distributions with a relative standard deviation of 5−12%, obtained from HRTEM analysis. Their size distribu-tion histograms are available in the Supporting Information.

Optical Properties and Alloying Analysis. Figure 2 shows the PL and absorption spectra for the Zn$_x$Cd$_{1-x}$Se nanocrystals with Zn mole fractions of 0, 0.28, 0.44, 0.55, and 0.67. In the absorption spectra, the first excitonic absorption wavelength decreases with the incorporation of ZnSe into the starting CdSe, while its overall shape remains similar. The first excitonic absorption peaks in the alloy nanocrystals are not as clear as those in binary CdSe nanocrystals. This poorly resolved absorption spectrum is characteristic of ternary Zn$_x$Cd$_{1-x}$Se nanocrystals, which is not caused by the wide size distribution.
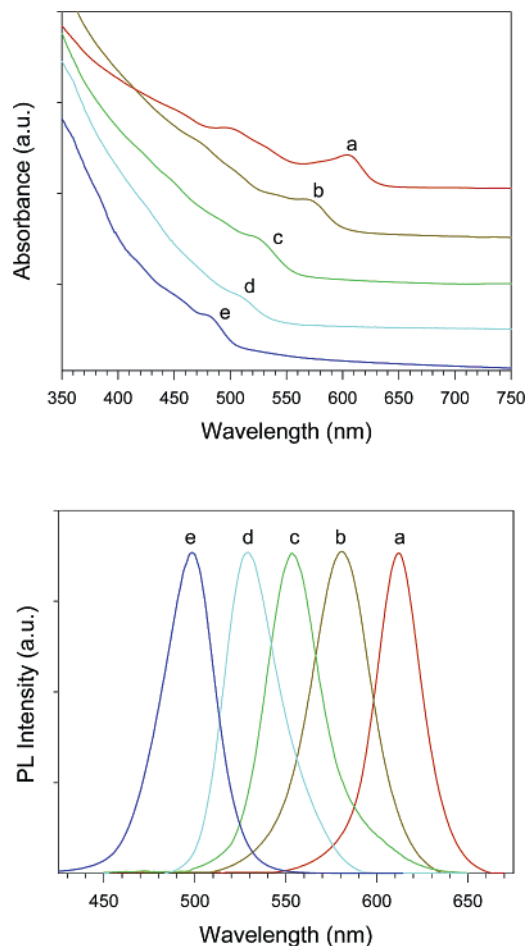

Figure 2. Absorption (top) and PL spectra with λ_{ex} = 365 nm (bottom) for the Zn$_x$Cd$_{1-x}$Se nanocrystals with Zn mole fractions of (a) 0, (b) 0.28, (c) 0.44, (d) 0.55, and (e) 0.67.

These nanocrystals have room-temperature emission efficiency ranging from 70% to 85% with full width at half-maximum (fwhm) of 22−30 nm, which is similar to that of the starting CdSe nanocrystals and comparable to the best result for the previously reported CdSe-based nanocrystals. With the increase of the Zn mole fraction from 0 to 0.67, a significant blue-shift of ∼110−120 nm was observed for both the first excitonic absorption onset and the band-edge luminescence peak of the nanocrystals (in the evolution of the emission color from red to blue).

The observed systematic composition-controlled shift of the absorption onset and emission maximum to shorter wavelength are explicable by the formation of Zn$_x$Cd$_{1-x}$Se composite nanocrystals via intermixing wider band-gap ZnSe with the narrower band-gap CdSe nanocrystals, rather than forming separate CdSe and ZnSe nanoparticles or core−shell structure CdSe/ZnSe. If ZnSe nucleated separately, the corresponding PL and absorption peaks should appear. This can rule out the formation of ZnSe nanocrystals, which is in agreement with the results of HRTEM measurement. If the CdSe/ZnSe core−shell QDs formed, the resulting absorption excitonic onset and emission maximum will shift to longer wavelength as compared with that of pure CdSe due to partial leakage of the exciton into the shell matrix (refer to alloying mechanism section).[14−17,26]

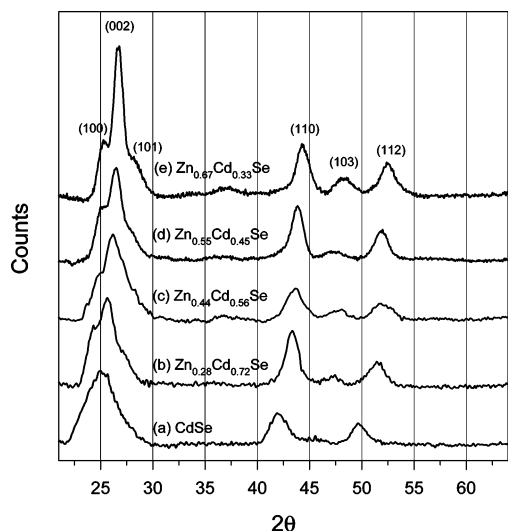(26) Danek, M.; Jensen, K. F.; Murray, C. B.; Bawendi, M. G. *Chem. Mater.* **1996**, *8*, 173.

Figure 3. X-ray powder diffraction patterns of $Zn_xCd_{1-x}Se$ nanocrystals with different Zn mole fractions of (a) 0, (b) 0.28, (c) 0.44, (d) 0.55, and (e) 0.67.

In the preparation of the $Zn_xCd_{1-x}Se$ nanocrystals, it was observed that the PL peak blue-shift-rate slowed gradually after finishing the addition of Zn and Se precursors. 3–6 min later, the PL peak profile (peak position and line width) was fixed, and retained for another 5–10 min. This gives an evidence for the homogeneous formation of $Zn_xCd_{1-x}Se$ alloy nanocrystals. If the nonideally mixed CdSe–ZnSe (involving CdSe and ZnSe domains, or a concentration gradient decreasing toward the dot interior) was formed, with the extension of heating time at high temperature, the two components should be further inter-diffused and composition will be more close to a $Zn_xCd_{1-x}Se$ alloy, resulting in the change of the PL peak profile (peak shape and position). If the band-gap energies of both bulk and nanocrystal $Zn_xCd_{1-x}Se$ are plotted against the Zn mole fractions,[27] a similar nonlinear relationship or bowing parameter was observed in the two systems (see the Supporting Information).

Figure 3 shows the XRD traces for the wurtzite $Zn_xCd_{1-x}Se$ compounds together with the indexing of major peaks. As the Zn content increases, the diffraction peaks gradually shift toward larger angles. The continuous peak shifting of the monodispersed nanocrystals may also rule out phase separation or separated nucleation of ZnSe nanocrystals. The enhanced intensity of the (002) reflection arising from preferred orientation is obvious due to the extended growth of (002) faces, in contrast to earlier studies where more rapid crystal growth along (002) leads to rodlike morphologies.[28,29] As we know, such a sharp peak is not available in core–shell structured QDs; thus it provides a direct method to more accurately determine the lattice spacing of $Zn_xCd_{1-x}Se$ nanocrystals. A gradual decrease in lattice spacing along the *c*-axis (from 7.01, 6.94, 6.80, 6.75, to 6.68 Å) is observed with the increase of Zn content in the nanocrystals. This trend is consistent with Vegard's law, which confirms the formation of alloy nanocrystals with homogeneous distribution of ZnSe inside the CdSe matrix.[30]

(27) Kolomiets, B. T.; Ling, C. M. *Sov. Phys.-Solid State* **1960**, *2*, 154.
(28) Manna, L.; Scher, E. C.; Li, L.-S.; Alivisatos, A. P. *J. Am. Chem. Soc.* **2002**, *124*, 7136.
(29) Peng, X.; Manna, L.; Yang, W. D.; Wickham, J.; Scher, E.; Kadavanich, A.; Alivisatos, A. P. *Nature* **2000**, *404*, 59.
(30) Furdyna, J. K. *J. Appl. Phys.* **1988**, *64*, R29.

Alloying Mechanism. To further study the alloying mechanism at the nanoscale, core–shell CdSe/ZnS, CdSe/CdS, and CdSe/ZnSe nanocrystals with a core size of 4.5 nm and shell thickness of 1–2 monolayers were prepared at temperatures below 220 °C according to the standard literature method.[15,16] The detailed procedure for the preparation of CdSe/ZnSe is provided in the Supporting Information. After the nanocrystals were heated at 300 °C for 10 min, only a small red-shift was observed in the CdSe/ZnS and CdSe/CdS due to particle growing via Ostwald ripening. However, a significant blue-shift of the PL peak was observed for the CdSe/ZnSe as expected, indicating the formation of $Zn_xCd_{1-x}Se$ nanocrystals. The two components CdSe and ZnSe in the CdSe/ZnSe differ only in the cations. But the two components in the CdSe/CdS and CdSe/ZnS differ either in the anions or in both the anions and the cations. As the group II cations diffuse much easier than the group VI anions in II–VI semiconductors,[31] the CdSe/ZnSe can be intermixed to form an alloy much easier than the CdSe/CdS or CdSe/ZnS. To study its alloying kinetics, the same batch of CdSe/ZnSe nanocrystals (PL wavelength at 580 nm) with core size of 4.5 nm and shell thickness of 1.1 monolayers was subjected to a 10-min heat treatment at different temperatures.

In the process of transforming the core–shell structured CdSe/ZnSe into alloyed $Zn_xCd_{1-x}Se$ nanocrystals, the evolution of the emission wavelength maximum of the resulting product as a function of temperature was measured as shown in Figure 4, where clear three-step (or region) alloying processes are observed: (i) a ripening process between 200 and 270 °C with a 7-nm red-shift of the PL peak from 580 to 587 nm for the core–shell nanocrystals; (ii) a rapid alloying process between 270 and 290 °C with a significant blue-shift of the PL peak from 580 to 548 nm (a sharp drop in the emission wavelength); and (iii) a stable region after the alloying step.

The alloying process starts to occur slowly at ~270 °C and speeds up considerably at further elevated temperatures. It can complete within 5 min when the temperature is higher than 290 °C. The results show that the core–shell structures are retained below 270 °C and transform into alloy rapidly above 270 °C. The very sharp boundary of temperature at 270 °C called "alloying point", analogous to melting or boiling points, is lower than the melting point of the alloy nanocrystals. This rapid alloying process at the nanoscale above the alloying point may be attributed to both the dramatic increase of the diffusion coefficient and the depression of the melting point as the particle size decreases.

For the synthesis of $Zn_xCd_{1-x}Se$ nanocrystals, a large excess of Se precursor was used to prepare the starting CdSe QDs, which may form a Se-rich surface.[15] This is helpful for the initial epitaxial growth of a very thin shell of ZnSe, which can alloy simultaneously with the CdSe QDs at high temperature via the internal self-diffusion. Certain amounts of Zn and Se precursors can be continuously supplemented the consumption of the ZnSe shell on the surface until the $Zn_xCd_{1-x}Se$ nanocrystals form.

PL Stability of Water-Soluble QDs. Next we studied the difference in the luminescence stability of mercaptoacetic acid capped CdSe/ZnS and $Zn_xCd_{1-x}Se$ nanocrystals in aqueous solutions.[6] Similar to the inorganic-passivated CdSe/ZnS nanocrystals, only a minor loss in the emission intensity was observed for the alloyed $Zn_xCd_{1-x}Se$ nanocrystals upon transfer from the

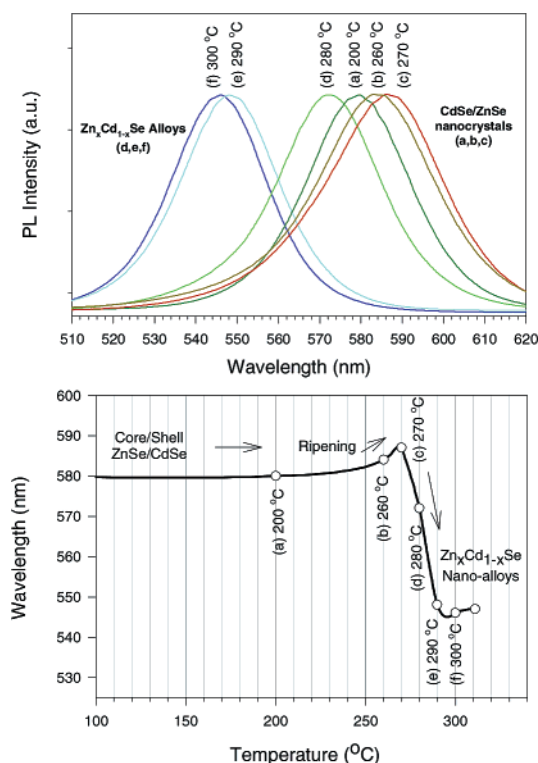(31) Shaw, D. *J. Cryst. Growth* **1988**, *86*, 778.

Figure 4. Evolution of the PL spectra in the progress of transforming CdSe/ZnSe core−shell nanocrystals (PL wavelength at 580 nm) to Zn$_x$Cd$_{1-x}$Se nanocrystals under the heat-treatment at different temperatures for 10 min each (top). The corresponding variation of PL wavelength as a function of heating temperature (middle). A schematic illustration of the kinetic alloying process from core−shell CdSe/ZnSe to alloyed Zn$_x$Cd$_{1-x}$Se nanocrystals (bottom).

organic phase into an aqueous solution. With the increase of the Zn content in the water-soluble Zn$_x$Cd$_{1-x}$Se nanocrystals, their emission efficiencies could be improved from 40% in the red spectral range to 55% in the blue emission window. Water-soluble CdSe/ZnS core−shell nanocrystals (∼4.0 nm in diameter with an emission wavelength at 550 nm) and water-soluble Zn$_{0.55}$Cd$_{0.45}$Se nanocrystals (∼6.8 nm in diameter with an emission at 529 nm) were heated separately at 80 °C in an air-saturated aqueous solution. For the alloy nanocrystals system, the PL intensity decreased only by less than 10% within 5-h treatment, and the PL peak shape and the emission wavelength maximum were remained (Figure 5). However, for the core−shell structured system, the PL intensity decreased by about 50% and the PL peak position red-shifted ∼10 nm after 5-h treatment.[8] During this process, the narrow symmetric emission peak profile was kept in the Zn$_{0.55}$Cd$_{0.45}$Se, but it became
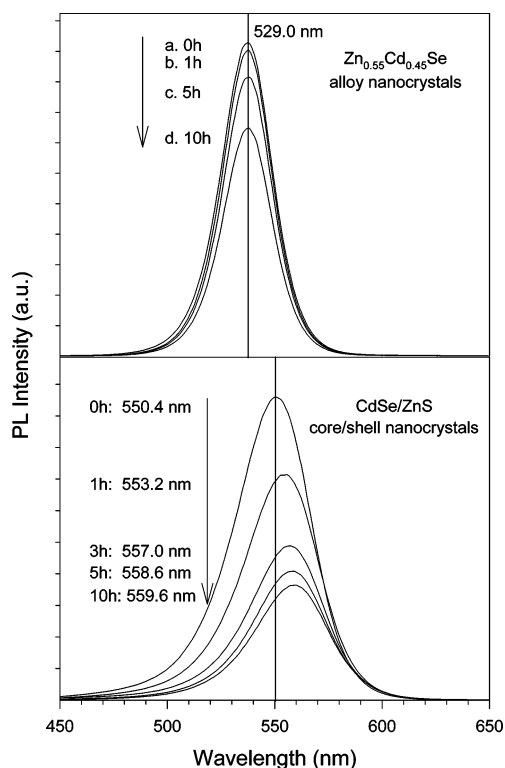

Figure 5. Time-dependent evolutions of the PL spectra of Zn$_{0.55}$Cd$_{0.45}$Se alloy nanocrystals (top) and CdSe/ZnS core−shell nanocrystals (bottom) in air-saturated aqueous solutions at 80 °C.

asymmetric in the CdSe/ZnS. Similar characteristics were confirmed for other color-emitting alloy nanocrystals. This unique feature of a fixed wavelength emission is independent of the rigorous environmental conditions. This character is very important for the accurate identification or quantitative analysis of biomolecules such as in PCR amplification applications.

Luminescence and Stability Discussion. A proven strategy for increasing the luminescence and stability of CdSe nanocrystals is to grow a thin inorganic layer of a wider band-gap semiconductor on the surface of the core nanocrystal. The high luminescence and stability of alloyed Zn$_x$Cd$_{1-x}$Se nanocrystals are attributable to the following factors:

(i) Larger particle size.[32,33] Larger sized QDs are more stable than smaller ones as smaller nanocrystals have a higher percentage of reactive surface atoms. Atoms on the surface are energetically less stable than those that are well ordered and packed in the interior. Larger nanocrystals have much weaker interactions with foreign species, which have less obvious influence on the overall electronic structure of the nanocrystals. However, a dramatic change in the electronic structure of smaller nanocrystals can be initiated by the interaction with foreign species. For the same color-emitting QDs, the Zn$_x$Cd$_{1-x}$Se nanocrystals have much larger sizes than the CdSe/ZnS nanocrystals. For example, blue-emitting Zn$_x$Cd$_{1-x}$Se nanocrystals have particle sizes of over 7-nm, which is ∼3 times larger than that of the blue-emitting CdSe/ZnS nanocrystals.

(ii) High crystallinity. Larger nanocrystals with complete lattice structure have much less defects. The extended growth

(32) Landes, C.; Braun, M.; Burda, C.; El-Sayed, M. A. *Nano Lett.* **2001**, *1*, 667.
(33) Landes, C. F.; Braun, M.; El-Sayed, M. A. *J. Phys. Chem. B* **2001**, *105*, 10554.

of (002) faces has less opportunity to form more stacking faults than the growth along (002) of nanorods does.

(iii) Hardened lattice structure and decreased inter-diffusion.[34,35] For $Zn_xCd_{1-x}Se$ nanocrystals, the weaker CdSe bond is stabilized by the stronger ZnSe bond, and the shorter bond length of ZnSe introduces stiff struts into the system, which lead to an increase of the dislocation energies.[34] The addition of ZnSe into the CdSe lattice results in an increased covalency and reduced ionicity, thus inhibiting plastic deformation and the generation of defects.[35] The hardened lattice of $Zn_xCd_{1-x}Se$ can reduce the higher self-diffusion of CdSe and thus counteract the creation of defects. A similar situation was observed in $Zn_xCd_{1-x}Te$ bulk materials, which have been successfully used as substrates in preference to CdTe for making infrared detectors because of their hardened lattice structure and lower dislocation densities.[35] Similarly, $Zn_xCd_{1-x}Se$ nano-alloys may have structural advantages over CdSe QDs.

(iv) Spatial composition fluctuation.[36,37] Inorganic-capped CdSe can provide a potential step for electrons and holes originating in the nanocrystals, and reduce the probability of the carriers to migrate the sample surface. However, spatial compositional fluctuations in $Zn_xCd_{1-x}Se$ nanocrystals can produce atomically abrupt jumps in the chemical potential that can further localize free exciton states in the alloy crystallites.

(34) Sher, A.; Chen, A.-B.; Spicer, W. E.; Shih, C.-K. *J. Vac. Sci. Technol.* **1985**, A3, 105.
(35) Bell, S. L.; Sen, S. *J. Vac. Sci. Technol.* **1985**, A3, 112.
(36) Strassburg, M.; Heitz, R.; Turck, V.; Rodt, S.; Pohl, U. W.; Hoffmann, A.; Bimberg, D.; Krestnikov, I. L.; Shchukin, V. A.; Ledentsov, N. N.; Alferov, Z. I.; Litvinov, D.; Rosenauer, A.; Gerthsen, D. *J. Electron Mater.* **1999**, *28*, 506.
(37) Korostelin, Y. V.; Shapkin, P. V.; Suslina, L. G.; Areshkin, A. G.; Markov, L. S.; Fedorov, D. L. *Solid State Commun.* **1989**, *69*, 789.

Summary

An effective synthetic method has been developed for the homogeneous formation of highly luminescent composition-tunable $Zn_xCd_{1-x}Se$ alloy nanocrystals, particularly with respect to the especially successful production of high-quality blue-emitting QDs. The emission wavelength across the visible spectrum can be tuned by changing the composition of the $Zn_xCd_{1-x}Se$ nanocrystals. A rapid alloying process occurs at the temperatures above the "alloying point". The high stability and luminescence of $Zn_xCd_{1-x}Se$ nanocrystals is attributed to the larger particle size, higher crystallinity, hardened lattice structure, lower interdiffusion, and spatial compositional fluctuation. These highly luminescent, stable alloy nanocrystals are potential ideal nano-emitters for light emitting devices or semiconductor lasers in optoelectronic applications. They are also very promising biological labels. We expect that this alloying method can be extended to synthesize high-quality alloy nanocrystals of other materials.

Supporting Information Available: The dependence of the band-gap energy E_g of bulk and alloyed nanocrystal $Zn_xCd_{1-x}Se$ as a function of compositions; size distribution histograms for all the samples; synthesis of core—shell CdSe/ZnSe nanocrystals. This material is available free of charge via the Internet at http://pubs.acs.org.

JA035096M